

# Excited states of exciton-polariton condensates in 2D and 1D harmonic traps

C. Trallero-Giner,<sup>1</sup> M. V. Durnev,<sup>2,3</sup> Y. Núñez Fernández,<sup>4</sup> M. I. Vasilevskiy,<sup>5</sup> V. López-Richard,<sup>6</sup> and A. Kavokin<sup>7</sup>

<sup>1</sup>*Facultad de Física, Universidad de La Habana, Vedado 10400, La Habana, Cuba*

<sup>2</sup>*Spin Optics Laboratory, State University of St-Petersburg, 1, Ulianovskaya, St-Petersburg, 19850, Russia*

<sup>3</sup>*Ioffe Physical-Technical Institute of the RAS, 194021 St.-Petersburg, Russia*

<sup>4</sup>*Centro Atómico de Bariloche, 8400, Argentina*

<sup>5</sup>*Centro de Física and Departamento de Física, Universidade do Minho, Campus de Gualtar, Braga 4710-057, Portugal*

<sup>6</sup>*Departamento de Física, Universidade Federal de São Carlos, 13.565-905, São Carlos, São Paulo, Brazil*

<sup>7</sup>*Physics and Astronomy School, University of Southampton, Highfield, Southampton, SO17 1BJ, UK and Spin Optics Laboratory, State University of St-Petersburg, 1, Ulianovskaya, St-Petersburg, 198504, Russia*

We present a theoretical description of Bogolyubov-type excitations of exciton-polariton Bose-Einstein condensates (BECs) in semiconductor microcavities. For a typical two dimensional (2D) BEC we focus on two limiting cases, the weak- and strong-coupling regimes, where a perturbation theory and the Thomas–Fermi approximation, respectively, are valid. We calculate integrated scattering intensity spectra for probing the collective excitations of the condensate in both considered limits. Moreover, in relation to recent experiments on optical modulation allowing localization of condensates in a trap with well controlled shape and dimensions, we study the quasi-one dimensional (1D) motion of the BEC in microwires and report the corresponding Bogolyubov’s excitation spectrum. We show that in 1D case the characteristic polariton-polariton interaction constant is expressed as  $g_1 = 3\lambda\mathcal{N}/(2L_y)$  ( $\lambda$  is the 2D polariton-polaritons interaction parameter in the cavity,  $\mathcal{N}$  the number of the particles, and  $L_y$  the wirecavity width). We reveal some interesting features for 2D and 1D Bogolyubov spectra for both repulsive ( $\lambda > 0$ ) and attractive ( $\lambda < 0$ ) interaction.

PACS numbers: 71.36.+c, 42.65.-k, 75.75.-c

## I. INTRODUCTION

The rich picture of the exciton-polariton Bose-Einstein condensates (BECs) in semiconductor microcavities has opened the opportunity for exploring a great variety of phenomena, such as superfluidity of quantum fluid<sup>1,2</sup>, vortices<sup>3</sup>, persistent currents<sup>4</sup>, half-quantum vortices<sup>5</sup>, as well as applications in quantum cascade laser<sup>6</sup> and interferometric devices (see Ref. 7 and references therein). The scheme of controlling the dynamic of condensates is ruled by their elementary excitations. The knowledge of the properties of these (Bogolyubov-type) excitations would reveal the main causes and allow for the detailed understanding of the physical phenomenon under consideration. Phonon-like excitation spectrum in the low-momentum regime of a quantum fluid condensate was firstly theoretically studied by Bogolyubov.<sup>8</sup> Finally, M. H. Anderson and co-workers<sup>9</sup> observed the Bogolyubov-de Gennes spectrum in a ultra-cold dilute atom cloud.

Polariton-polariton interaction and the behavior of the excitation spectra play a fundamental role for understanding the underlying physics of the BEC dynamic in semiconductor microcavities. Utsunomiya *et.al* have realized<sup>10</sup> the first experimental observation of Bogolyubov spectrum in a GaAs/AlGaAs microcavity by showing, in the phonon-like regime, a clear linearization of the quadratic polariton dispersion as a function of the in-plane wavevector  $\mathbf{k}$ . This tendency was later observed in Ref. 11, along with an indication that the excitation spectrum becomes diffusive (dispersionless at low momenta) if the condensate is driven far from equilibrium. Neverthe-

less, the exciton-polariton excitation energy is modified if the condensate is loaded in a 2D trap potential, thus the spectrum of collective excitations must be characterized by appropriate quantum numbers describing the confined phonon-like excitations.

In addition to the two-dimensional nature of the BEC in semiconductor microcavities, a dynamical condensation of exciton-polaritons can also be induced in one-dimensional (1D) systems. Nowadays, it is possible to realize and manipulate diverse trap potentials for exciton-polaritons.<sup>7,12–14</sup> This experimental ability enhances the range of potential applications, such as the design of condensate circuits,<sup>7</sup> among others. In particular, 1D parabolic confined potentials can be generated in microwires or by optical manipulation. Then, optical modulation allows to control the shape of the condensate wave functions and to study their quasi-1D motion in the microcavity.<sup>13,15</sup> In particular, exciton-polariton 1D harmonic traps have been induced by employing two pump laser beams.<sup>7,16</sup>

The aim of this paper is to give a mathematical description of elementary excitations of a confined BEC in microcavities, with a special emphasis on the shape and dimensionality of the trap potentials. We explore convenient analytical descriptions of the condensate that can be used to study its dynamics and related physical phenomena, such as vortices, persistent currents and superfluidity. In this work we limit ourselves by considering a condensate where the inward flux of polaritons is exactly balanced by their decay out of the cavity. Extension to out-of-equilibrium condensates is possible by considering the complex Gross-Pitaevskii equation, in which case the

elementary excitation frequencies become complex and are to be found numerically.<sup>17</sup>

The article is organized as follows. Section II is devoted to the Bogolyubov-type elementary excitations in a 2D parabolic potential. Two approaches are discussed: (i) a perturbative method where the cubic term present in the non-linear Gross-Pitaevskii equation (GPE), can be considered as perturbation in comparison to the trap potential, and (ii) the so-called strong coupling regime or Thomas-Fermi limit where the collective excitations of the ground state are described by the variation of its density. Also, we report calculated spectra of electromagnetic waves scattered by the condensate comparing both limits of weak and strong non-linear interactions. In Sec. III, we first deal with the reduction of the spatial 2D GPE to an effective 1D equation by "freezing" the transversal direction if the cavity width is much smaller than the harmonic oscillator length. The procedure allows us to rigorously obtain the effective 1D polariton-polariton interaction constant. Then, in the framework of the present model, we derive the Bogolyubov excitations for the 1D parabolic and semi-parabolic traps and show the main differences between them. Finally, in Sec. IV is devoted to conclusions.

## II. TWO DIMENSIONAL COLLECTIVE EXCITATIONS

Within the framework of the mean field theory, the physical characteristics of a trapped BEC described by a macroscopic wave function  $\Psi(\mathbf{r}, t)$  are ruled by the time dependent 2D nonlinear GPE,

$$i\hbar\partial_t\Psi = \left(-\frac{\hbar^2}{2m_*}\Delta + V(\mathbf{r}) + \lambda|\Psi|^2\right)\Psi, \quad (1)$$

where  $\mathbf{r} = (r, \theta)$  is the radius vector in polar coordinates,  $\lambda$  is the self-interaction parameter,<sup>18,19</sup>  $m_*$  is the exciton-polariton mass, and  $V(\mathbf{r}) = m_*(\omega_{0x}^2x^2 + \omega_{0y}^2y^2)/2$  is the two dimensional harmonic potential characterized by the trap frequencies  $\omega_{0x}, \omega_{0y}$ .

The collective excitations can be obtained by applying a small deviation from the stationary solutions  $\Psi_0(\mathbf{r}, t) = \psi_0(\mathbf{r})\exp(-i\mu t/\hbar)$  of Eq. (1) in the form of<sup>20</sup>

$$\Psi(\mathbf{r}, t) = \exp(-i\mu t/\hbar) [\psi_0(\mathbf{r}) + u(\mathbf{r})\exp(-i\omega t) + v^*(\mathbf{r})\exp(i\omega t)], \quad (2)$$

where  $\mu$  is the chemical potential,  $u$  and  $v$  are the amplitudes of the excitation mode with frequency  $\omega$ . The perturbative nature of the last two terms in Eq. (2) is ensured if the following conditions are satisfied,  $\langle u|u\rangle, \langle v|v\rangle \ll \langle \psi_0|\psi_0\rangle$ . After substituting the perturbed wave function (2) into Eq. (1) and performing the linearization procedure, one obtains the following eigenvalue problem for the frequencies  $\omega$  and amplitudes  $u$

and  $v$ :

$$\begin{bmatrix} -\frac{\hbar^2}{2m_*}\Delta + U(\mathbf{r}) & \lambda|\psi_0|^2 \\ -\lambda|\psi_0|^2 & \frac{\hbar^2}{2m_*}\Delta - U(\mathbf{r}) \end{bmatrix} \begin{pmatrix} u \\ v \end{pmatrix} = \hbar\omega \begin{pmatrix} u \\ v \end{pmatrix}, \quad (3)$$

with

$$U(\mathbf{r}) = V(\mathbf{r}) + 2\lambda|\psi_0(\mathbf{r})|^2 - \mu. \quad (4)$$

The operator in Eq. (3) is not Hermitian, however, its spectrum lies entirely in real space<sup>21</sup> with the set of positive and negative values  $\omega$  corresponding to  $(u : v)^T$  and  $(v^* : u^*)^T$  states, respectively. The ground state characteristics  $\psi_0$  and  $\mu$  can be found from the stationary GPE

$$\left(-\frac{\hbar^2}{2m_*}\Delta + V(\mathbf{r}) + \lambda|\psi_0|^2\right)\psi_0 = \mu\psi_0, \quad (5)$$

with the boundary conditions  $\psi_0 \rightarrow 0$  at  $r \rightarrow \infty$  and normalized over the total number of condensed particles,  $\mathcal{N}$ ,

$$\langle \psi_0 | \psi_0 \rangle = \int |\psi_0(\mathbf{r})|^2 d\mathbf{r} = \mathcal{N}. \quad (6)$$

Let us now introduce the dimensionless parameter  $\Lambda = \lambda m_* \mathcal{N} / \hbar^2$  which describes the strength of interaction in the system. We will further focus on the two important limiting cases when solutions of Eqs. (3) and (5) can be found analytically, namely, the limits of sufficiently small and large values of  $\Lambda$ . In the former limit the interaction term can be treated in the framework of the perturbation theory while in the latter case (the so-called Thomas-Fermi approximation) collective excitations are the solutions of the hydrodynamic-like equations.<sup>22</sup>

### A. Perturbative method

As known, the polariton-polariton self-interaction parameter  $\lambda$  depends on exciton-photon detuning  $\delta$ .<sup>19</sup> For typical GaAs/AlGaAs microcavities, the perturbation theory for the GPE (5) is valid if the number of particles in the condensate  $\mathcal{N} \leq 10^4$  for  $-10 \text{ meV} < \delta < 3 \text{ meV}$  or  $\mathcal{N} \leq 10^6$  if the detuning lies in the interval  $3 \text{ meV} < \delta < 7 \text{ meV}$ .<sup>23</sup> All these cases correspond to the dimensionless self-interaction coefficient's values  $-3 < \Lambda < 3$ .<sup>18</sup> In this range of parameter  $\lambda$ , the nonlinear term  $\lambda|\psi_0|^2$  in Eq. (5) can be considered as a small perturbation with respect to the isotropic ( $\omega_{0x} = \omega_{0y} = \omega_0$ ) harmonic trap confinement potential,  $m_*\omega_0^2 r^2/2$ . Hence, the order parameter  $\psi_0$  can be expanded in series of the complete set of 2D harmonic oscillator wave functions<sup>23</sup>

$$\varphi_{N,m_z}(\rho, \theta) = \frac{\exp(im_z\theta)}{\sqrt{2\pi}} R_{N,m}(\rho), \quad (7)$$

with  $\rho = r/a$ ,  $a = \sqrt{\hbar/m_*\omega_0}$  the characteristic unit length,  $m_z$  the  $z$ -projection of the angular momentum,  $m = |m_z|$ , and  $N = 0, 1, 2, \dots$ . The corresponding energies measured in units of  $\hbar\omega_0$  are  $\epsilon_N = N + 1$ .

The chemical potential and the condensate distribution  $n_0 = |\psi_0|^2$  up to the second and first order in  $\Lambda$  read<sup>18</sup>

$$\frac{\mu}{\hbar\omega_0} = 1 + \frac{\Lambda}{2\pi} - \frac{3\Lambda^2}{8\pi^2} \ln(4/3), \quad (8)$$

$$\begin{aligned} n_0(r) &= \frac{\overline{n_0(\rho)}}{a^2} = \frac{n^{(0)} + \Lambda n^{(1)}}{a^2} \\ &= \frac{1}{\pi a^2} \exp(-\rho^2) [1 + \Lambda F(\rho)], \end{aligned} \quad (9)$$

with

$$F(\rho) = \frac{1}{2\pi} [\gamma + \ln(\rho^2/2) + \Gamma(0, -\rho^2)]. \quad (10)$$

Here  $\Gamma(0, z)$  is the incomplete gamma function and  $\gamma$  is the Euler-Mascheroni constant.<sup>24</sup> Since the perturbation,  $\lambda|\psi_0|^2$ , in Eq. (3) does not mix states with different angular momenta  $m = |m_z|$ , we can search the required solutions as  $u[v] = \exp(im_z\theta)u_{N,m}(\rho)[v_{N,m}(\rho)]/\sqrt{2\pi}$  with the amplitudes  $u_{N,m}$  and  $v_{N,m}$  expanded over the set of 2D radial components of oscillator wave functions  $\{R_{N,m}\}$ ,

$$\begin{pmatrix} u_{N,m} \\ v_{N,m} \end{pmatrix} = \sum_{N_1=0}^{\infty} \begin{pmatrix} A_{NN_1} R_{N_1,m} \\ B_{NN_1} R_{N_1,m} \end{pmatrix}. \quad (11)$$

Substituting Eq. (11) into Eq. (3), one can obtain the spectrum of the Bogolyubov's excitations (see Appendix A for details). It is possible to show that  $\omega_{N,m}$  up to the second order in  $\Lambda$  can be cast as

$$\omega_{N,m} = \omega_0 \left( N + \Lambda \varpi_{N,m}^{(1)} + \Lambda^2 \varpi_{N,m}^{(2)} \right), \quad (12)$$

where the coefficients  $\varpi_{N,m}^{(1)}$  and  $\varpi_{N,m}^{(2)}$  are obtained in the Appendix A.

Figure 1 displays the excitation frequencies  $\omega_{N,m}$  for the lowest 11 collective modes *versus* the dimensionless interaction parameter  $\Lambda$ . Let us note that the excitation frequencies in the non-interacting limit are equal to those of the two-dimensional harmonic oscillator measured from the zero-level  $\omega_0$  oscillations. At  $\Lambda = 0$ , the system is  $(N+1)$  degenerate with respect to angular momentum value  $m_z$ , which is a direct consequence of the axial symmetry inherent to the isotropic 2D harmonic confinement potential. At  $\Lambda \neq 0$ , the frequency corrections  $\varpi_{N,m}^{(1)}$  and  $\varpi_{N,m}^{(2)}$  depend on  $m$  (see Eqs. (A7) and (A11), respectively). Hence, the non-linear perturbative term splits the energy spectrum by the absolute value of the angular momenta projection  $m$ , leaving the two-fold degeneracy with respect to the sign of  $m_z$ . Figure 1

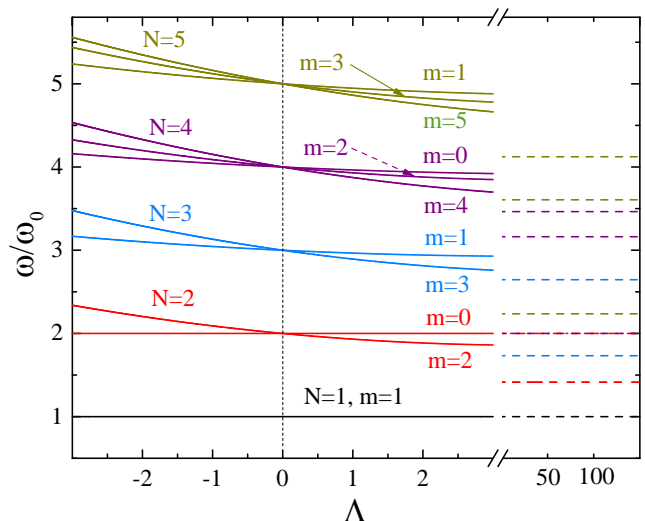


FIG. 1. (Color online): Excitation spectrum  $\omega_{N,m}$  as a function of the reduced self-interaction parameter  $\Lambda$ . Solid lines: Bogolyubov's spectrum solution of Eq. (12). Dashed lines: Thomas-Fermi approximation after Eq. (21).

shows that for the repulsive interaction, the excitation energies decrease with the increase of the condensate density. From the figure it follows that the doubly degenerate dipole excitation states  $N = 1, m_z = \pm 1$  (mode  $\omega_{1,1}$ ) are unaffected by the nonlinear interaction. This mode is harmonic, in agreement with the Kohn's theorem,<sup>25</sup> and it represents a rigid motion of the center of mass.<sup>22,26</sup> Notice that the same result holds under Thomas-Fermi limit in the framework of the hydrodynamic approximation as it is represented by dashed lines in Fig. 1. For the attractive potential, the excitation energy  $\omega_{N,m}(\Lambda < 0)$  increases as  $\Lambda$  decreases and, for a given radial quantum number  $N$ , the lower value of  $\omega_{N,m}(\Lambda < 0)$  corresponds to the lower quantum number  $m$ . Notice that in the case of repulsive interaction the opposite trend is obtained, i.e.  $\omega_{N,m}$  decreases as  $\Lambda$  increases and  $\omega_{N,m}(\Lambda > 0) > \omega_{N,m+2}(\Lambda > 0)$ . The amplitudes  $u_{N,m}$  and  $v_{N,m}$  up to first order in  $\Lambda$  are given in Appendix A. For a clearer demonstration of the space distribution of excitations, we evaluate the density function excited particles distribution  $D_{exc} = -\text{Im} \left\{ \text{Tr} \left[ \hat{G}(\mathbf{r}, \mathbf{r}; \omega) \right] \right\}$ , where  $\hat{G}(\mathbf{r}, \mathbf{r}; \omega)$  is the matrix Green's function of the Eq. (3) given by

$$\hat{G}(\mathbf{r}, \mathbf{r}'; \omega) = \frac{1}{\hbar} \sum_{N, m_z} \frac{[\hat{\chi}_{N, m_z}(\mathbf{r})]^T \hat{\chi}_{N, m_z}^*(\mathbf{r}')}{\omega - \omega_{N, m} + i\gamma_d}. \quad (13)$$

Here  $\hat{\chi}_{N, m_z}(\mathbf{r}) = [u_{N, m}(r)e^{im_z\theta} : v_{N, m}(r)e^{im_z\theta}]$  and  $\gamma_d$  is the damping parameter of the photon mode in the microcavity. The summation in Eq. (13) is performed only over  $N$  while the value of  $m_z$  is set constant,  $m_z = 0$ . In Fig. 2 the calculated exciton-polariton density distribution  $D_{exc}(\mathbf{r}; \omega)$  is shown for  $\Lambda = 1$ , and  $\gamma_d = 0.1\omega_0$ . The bright spots observed in the figure correspond to the

minima of the excitation density and are linked to the zeros of the radial density function  $|R_{N,m=0}(\rho)|^2$ , i.e. for a given  $\omega_{N,m=0}$  the function  $D_{exc}$  has  $n = N/2$  minimum in space domain.

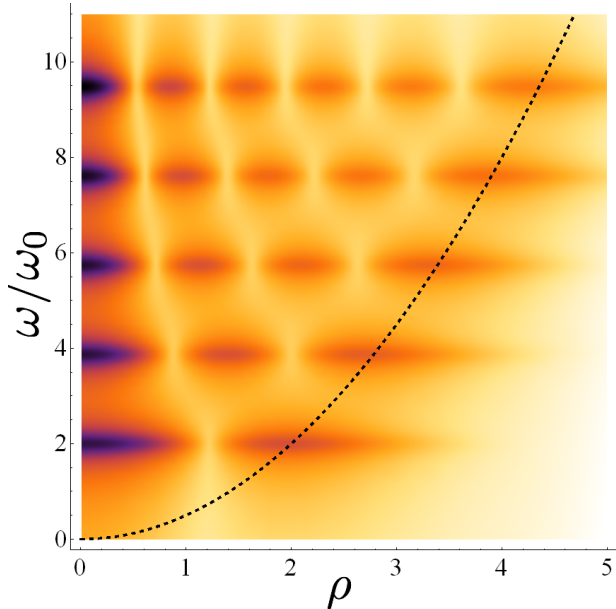


FIG. 2. (Color online): Calculated frequency-coordinate space distribution function,  $D_{exc}(\mathbf{r};\omega)$ , of the Bogolyubov collective excitation (see text) in a 2D parabolic trap. The parameter used are:  $m = 0$ ,  $\Lambda = 1$  and  $\gamma_d = 0.1\omega_0$ . The dark dot curve shows the dimensionless harmonic potential  $V(r)/\omega_0 = \rho^2/2$ .

### B. Current density

Superfluidity, the formation of quantized vortices,<sup>28</sup> and persistent currents<sup>4</sup> are among the most interesting properties of exciton-polariton condensates. Collective fluid dynamics of condensates can be driven coherently by the continuous-wave pump energy and triggered by a short pulse of another laser.<sup>1</sup> Also, vortices can be excited by a pulsed probe transferring angular momentum resonantly with the pumping signal.<sup>4</sup> In all considered effects, and in a general sense, assessing the current density,  $\mathbf{j}(\mathbf{r}, t)$ , becomes necessary and the evolution of the density profile for the collective excitations is of interest. Starting from the well known equation for the current density,

$$\mathbf{j}_{N,m_z} = \frac{\hbar}{2mi} [\Psi_{N,m_z}^* \nabla \Psi_{N,m_z} - (\nabla \Psi_{N,m_z}^*) \Psi_{N,m_z}] \quad (14)$$

and rewriting the wave function as  $\Psi_{N,m_z}(\mathbf{r}, t) = |\Psi_{N,m_z}(\mathbf{r}, t)| \exp(iS_{N,m_z}(\mathbf{r}, t))$  we obtain:

$$\mathbf{j}_{N,m_z}(\mathbf{r}, t) = c_{N,m_z}(r, t) \mathbf{v}_s(\mathbf{r}, t), \quad (15)$$

where  $\mathbf{v}_s(\mathbf{r}, t) = \frac{\hbar}{m} \nabla S(\mathbf{r}, t)$  is known as the superfluid velocity. Notice that integer vortices are described by rotation of  $S \rightarrow S + 2\pi p$ , with  $p = \pm 1, \pm 2, \dots$  and half vortices correspond to  $p = \pm 1/2, \pm 3/2, \dots$ <sup>5</sup> In Eq. (15),  $c_{N,m_z}(r, t) = |\Psi_{N,m_z}|^2 = |\psi_0(\mathbf{r}, t) + \delta\Psi_{N,m_z}(\mathbf{r}, t)|^2$  represents the total concentration of particles in the excited state  $(N, m_z)$ .

The non-zero  $\theta$ -component of the current density associated with an elementary excitation is obtained by evaluating the gradient,

$$j_{N,m_z}^\theta(\mathbf{r}, t) = \frac{m_z \hbar}{2m_*} \delta c_{N,m_z}(r, t), \quad (16)$$

where the condensate density perturbation,  $\delta c_{N,m_z}$ , is given by:

$$\begin{aligned} \delta c_{N,m_z} &= |\Psi_{N,m_z}(\rho, t)|^2 - |\psi_0(\rho, t)|^2 = \\ &= \sqrt{\frac{2}{\pi}} \cos(\omega_{N,m} t - m_z \theta) \left[ \psi_0 R_{N,m} + \frac{2}{\sqrt{\pi}} \Lambda \exp(-\rho^2/2) \times \right. \\ &\quad \left. \sum_{N_2 \neq N} C_{N,N_2,m}^{(0)} R_{N_2,m} \frac{N + 3N_2}{(N - N_2)(N + N_2)} \right]. \quad (17) \end{aligned}$$

The excitation density profiles  $\delta c_{N,m}$  at  $t = 0$  are displayed in Fig. 3 for  $(N = 1, m_z = 1)$ ,  $(N = 7, m_z = 3)$ , and  $(N = 6, m_z = 0)$ . Figure 3 illustrates the symmetry properties of the excited states as a function of the quantum number  $m_z$ . Since  $\delta c_{N,m}(t = 0) \sim \cos(m_z \theta)$  the profile shows the nodal distribution at  $\theta_p = (2p + 1) \pi / (2m_z)$  with  $p = 0, 1, \dots, |m_z|$ .

### C. Thomas-Fermi limit

For sufficiently large values of parameter  $\Lambda$ , the density profile of the condensate becomes smooth enough to omit the kinetic energy term in Eq. (5).<sup>29</sup> We then arrive to the so-called Thomas-Fermi limit with the ground state density,

$$n_{0TF}(\mathbf{r}) = \begin{cases} \frac{\mu_{TF}}{\hbar\omega_0} \frac{1}{\Lambda} \left(1 - \frac{r^2}{r_0^2}\right), & r < r_0; \\ 0, & r \geq r_0. \end{cases} \quad (18)$$

Here  $r_0 = \sqrt{2\mu_{TF}/(m_*\omega_0^2)}$  is the radius of the condensate ground state in the Thomas-Fermi limit. The normalization condition (6) yields for the chemical potential  $\mu_{TF} = \hbar\omega_0 \sqrt{\Lambda/\pi}$  so that  $\mu_{TF}$  is large compared to the oscillator energy. For the collective excitations we follow the approach developed in Ref. 22 for atomic condensates in three dimensional traps, which can be directly applied to the 2D case. Rather than considering small deviations of the wave function, let us now describe the collective excitations of the ground state by the variation of its density  $\delta c_{TF}(\mathbf{r}, t) = \delta c_{TF}(\mathbf{r}) = [n(\mathbf{r}) - n_{0TF}(\mathbf{r})] e^{i\omega_{TF} t}$  and frequency  $\omega_{TF}$ . The equation for  $\delta c_{TF}$  can be derived after some transformation of the GPE including the



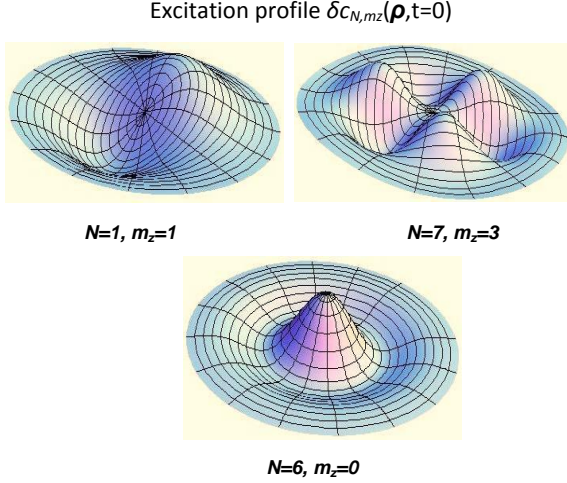


FIG. 3. (Color online): Excitation profile  $\delta c_{N,m}$  given by Eq. (17) at  $t = 0$  for the excited states ( $N = 1, m_z = 1$ ), ( $N = 7, m_z = 3$ ) and ( $N = 6, m_z = 0$ ). Here  $\Lambda = 1$ .

linearization procedure and omitting the kinetic energy terms. We then finally arrive to the following hydrodynamic equation:

$$\omega^2 \delta c_{TF} = -\frac{1}{2} \omega_0^2 \nabla (r_0^2 - r^2) \nabla \delta c_{TF}, \quad (19)$$

defined in the same region as Eq. (5). The solution of (19) can be cast as

$$\delta c_{TF}(\mathbf{r})_{n,m_z} = P_{2n,m}(r/r_0) (r/r_0)^m e^{im_z \varphi}, \quad (20)$$

where  $P_{2n,m}(x) = \sum_{k=0}^{k=n} d_{2k} x^{2k}$  and the coefficients  $d_{2k}$  satisfy the recurrence relation

$$d_{2k+2} = d_{2k} \frac{(n+m+k+1)(k-n)}{(m+k+1)(k+1)}$$

for  $k = 0, 1, \dots$  and  $d_0 = 1$ . The dispersion relation for the excitation modes is given by the formula (cf. Ref. (22))

$$\omega_{TFn,m} = \omega_0 \sqrt{2n^2 + 2n + 2nm + m}. \quad (21)$$

Following the same trends as in the 3D case (see Ref. 20) in the limit of strong particle interactions, the excitation energies become  $\Lambda$  independent. This result is represented in Fig. 1 by dashed lines. One can see again that the frequencies of the dipole mode ( $n = 0, m = 1$ )  $\omega_{TFn=0,m=1} = \omega_0$  in the Thomas-Fermi and perturbative approaches indeed coincide. Moreover, the excited state  $N = 2, m_z = 0$  in both considered limits is also harmonic, i.e.  $\omega_{N=2,m=0} = \omega_{TFn=1,m=0} = 2\omega_0$ .

#### D. Probing the excited states of the condensate

Light scattering spectroscopy is a common technique for investigation of the optical properties of semiconductors,<sup>27,30,31</sup> which can be used for probing the excited

states of the Bose-Einstein condensates in microcavities. Consider the two dimensional exciton-photon system in the strong coupling regime probed by a low-intensity resonant electromagnetic wave. The scattered wave can be found within the so called input-output approach<sup>32,33</sup>. The internal polariton modes are resonantly excited by the incident field so that Eq. (1) gains an additional ‘‘pump’’ term and can be written as<sup>32</sup>

$$i\hbar \partial_t \Psi = \left( -\frac{\hbar^2}{2m_*} \Delta + V(\mathbf{r}) + \lambda |\Psi|^2 \right) \Psi + \gamma_d t_A E(\mathbf{r}, t). \quad (22)$$

Here  $E(\mathbf{r}, t)$  is the incident field, which can be written as  $E = E_0 e^{i\mathbf{k}\mathbf{r}} e^{-i\mu t/\hbar} \cos \omega t$ ,  $\mathbf{k}$  is the in-plane wave vector ( $\mathbf{k} = 0$  under normal incidence),  $\gamma_d$  is the cavity damping parameter, and  $t_A$  is the amplitude transition coefficient of the cavity mirrors. The wave function  $\Psi$  should be treated as the polarization of an exciton mode or the electric field of a photon mode. Substituting in Eq. (22) the wave function in the form (2) yields the problem identical to Eq. (3) but with a nonzero right part  $[-1/2tE_0 e^{i\mathbf{k}\mathbf{r}} : 1/2tE_0 e^{i\mathbf{k}\mathbf{r}}]^T$ . Using the Green’s function formalism (13), the solution of this non-uniform problem is readily obtained. Therefore the output (scattered) field in the positive frequency range can be written as

$$E_{\text{out}}(\mathbf{r}) \propto t_A^* \Psi = \frac{1}{2} |t_A|^2 \gamma_d E_0 e^{-i\frac{\mu}{\hbar} t} \sum_{N,m} \frac{\varkappa_{N,m_z} u_{N,m_z}(r) e^{im_z \theta}}{\hbar (\omega_{N,m} - i\gamma_d - \omega)} e^{-i\omega_{N,m} t}, \quad (23)$$

$$\varkappa_{N,m}(\mathbf{k}) = \frac{1}{2\pi} \int [u_{N,m_z}^* - v_{N,m_z}^*] e^{-im_z \theta'} e^{i\mathbf{k}\mathbf{r}'} d\mathbf{r}'.$$

A possible experimental observable is the integrated intensity of the scattered wave given by

$$\frac{4 \int |E_{\text{out}}(\mathbf{r})|^2 d\mathbf{r}}{|t_A|^4 E_0^2} = \gamma_d^2 \sum_{N,m_z} \frac{|\varkappa_{N,m_z}|^2}{\hbar^2 [(\omega_{N,m} - \omega)^2 + \gamma_d^2]}. \quad (24)$$

This quantity is represented in Fig. 4(a) for different values of the wave vector  $\mathbf{k}$  (corresponding to different angles of incidence of the probing wave). One can see that at normal incidence ( $k = 0$ ) only the modes with  $m = 0$  are excited and due to parity considerations the modes with even radial numbers  $n$  exhibit considerably stronger interaction with the probing field. At  $k \neq 0$  the modes with non-zero  $m$  appear and the peak value shifts towards higher energies with increasing  $k$ .

In the Thomas-Fermi limit, the expression for the field analogous to Eq. (23) is obtained if one takes the wave functions of excitations in the form of  $\delta c_{TF}(\mathbf{r})_{n,m_z} / \sqrt{n_{0TF}(\mathbf{r})}$ . The scattered spectrum then has the same form as given by Eq. (24) with the following  $\varkappa_{N,m_z}$  coefficients:

$$\varkappa_{n,m_z}(\mathbf{k}) = \int \frac{\delta c_{TF}(\mathbf{r}')_{n,m_z}}{\sqrt{c_{0TF}(\mathbf{r}')}} e^{-im_z \theta'} e^{i\mathbf{k}\mathbf{r}'} d\mathbf{r}'. \quad (25)$$

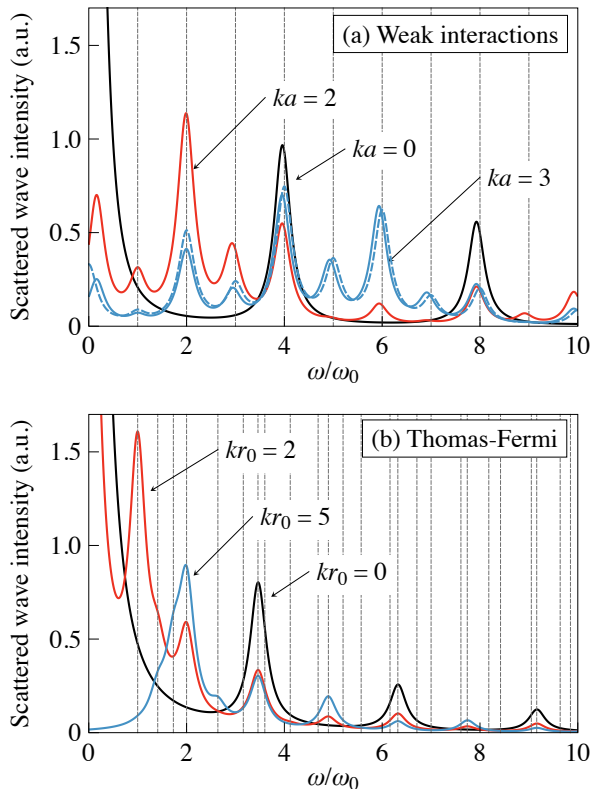


FIG. 4. (Color online): Spectra of the scattered field in the limit of weak (a) and strong (b) interactions. Dashed vertical lines indicate the frequencies calculated by Eq. (12) at  $\Lambda = 0$  (a) and by Eq. (21) (b). For comparison, the spectrum at  $ka = 3$  and  $\Lambda = 0$  is shown in panel (a) by the dashed curve.

The calculated spectra are presented in Fig. 4(b).

### III. QUASI ONE-DIMENSIONAL EXCITON-POLARITON CONDENSATES

In the following, we reduce the two dimensional GPE (1) to a 1D problem along the axial direction ( $x$ ) of a microwire. This can be done by "freezing out" the  $y$ -motion of the condensate (due to the presence of a lateral confinement potential) and by re-normalizing the mean-field interaction. We consider a wire cavity with a separable potential  $V(\mathbf{r}) = U_x(x) + U_y(y)$ , where  $U_x(x) = \frac{1}{2}m\omega_{0y}x^2$  is the harmonic trap and  $U_y$  is the cavity confinement potential along  $y$ -axis. Employing the adiabatic approximation, the order parameter  $\Psi(\mathbf{r}, t)$  can be factorized as

$$\Psi(\mathbf{r}, t) = \sqrt{N}\phi_x(x, t) \exp(-iE_y t/\hbar)\phi_y(y), \quad (26)$$

where the longitudinal wave function  $\phi_y$  and the energy  $E_y$  are determined by the auxiliary problem

$$E_y \phi_y = \left[ \frac{p_y^2}{2m_*} + U_y \right] \phi_y.$$

Assuming an infinite confinement barrier, the polariton eigenenergies are  $E_y = \hbar\omega_{n_y}$  with  $\omega_{n_y} = \frac{\hbar}{2m} \left( \frac{n_y\pi}{L_y} \right)^2$ ,  $n_y$  is an integer number, and  $L_y$  denotes the microwire cavity length. (Notice that the adiabatic approximation is restricted to the strong spatial confinement case where the frequency  $\omega_{0x} \ll \omega_{n_y=1}$ ). Substituting Eq. (26) into Eq. (1) and assuming that the condensate along the  $y$ -direction remains close to the  $\omega_{n_y=1}$  ground state with  $\phi_{n_y=1} = \sqrt{2/L_y} \sin(\pi x/L_y)$ , we obtain the equation<sup>34</sup>

$$i\hbar\partial_t\phi_x = \left( \frac{p_x^2}{2m_*} + U_x + g_1|\phi_x|^2 \right) \phi_x, \quad (27)$$

where  $g_1 = 3\lambda\mathcal{N}/(2L_y)$  is the effective 1D polariton-polariton interaction constant.<sup>36</sup>

#### A. Normal modes in 1D-parabolic potential

In this case, we employ the same method of the linear response as in Section II with  $V(\mathbf{r}) \rightarrow m_*\omega_{0x}^2x^2/2$ ,  $\Lambda \rightarrow \Lambda_{1D} = g_1/(l_x\hbar\omega_{0x})$ , and  $l_x = \sqrt{\hbar/(m_*\omega_{0x})}$ . The present problem is analogous to the one studied for diluted atomic gases in 1D optical lattices (see Refs. 37 and 38). Applying those results to our case we have for the 1D chemical potential:

$$\mu_{1D} = \omega_{0x} \left( \frac{1}{2} + \frac{\Lambda_{1D}}{\sqrt{2\pi}} + C_1\Lambda_{1D}^2 \right) \quad (28)$$

and for the 1D excitation frequencies,

$$\omega_k^{(1D)} = \omega_{0x} \left[ k + \frac{\Lambda_{1D}}{\sqrt{2\pi}} \left( -1 + \frac{2\Gamma(k+1/2)}{\sqrt{\pi}k!} \right) \right. \\ \left. \Lambda_{1D}^2 \left( \frac{\gamma_k}{2\pi^2} - C_1 \right) \right]; \quad k = 1, 2, \dots, \quad (29)$$

where  $C_1 = \frac{3}{2\pi} \ln \left[ \frac{\sqrt{3}}{4} + \frac{1}{2} \right]$ ,  $\Gamma(z)$  is the gamma function and  $\gamma_k$  are numeric parameters given elsewhere.<sup>38</sup> The corresponding total density in the excited state  $k$ ,  $c_k^{(1D)}(x, t)$ , and the excitation profile,  $\delta c_k^{(1D)}(x, t)$  are displayed in the Appendix B.

The dynamics of the condensate calculated using Eqs. (B1)-(B3) are sketched in Fig. 5 by a 2D map of the density,  $c_k^{(1D)}(x, t)$  ( $k = 2$  and 3) as function of dimensionless coordinate  $x/l_x$  and time  $t\omega_{0x}$ . For the calculation we chose  $\Lambda_{1D} = \pm 2$ . From the figure we observe that, for a certain moment of time, there are pronounced oscillations of the density,  $c_k^{(1D)}(x, t)$ , along the

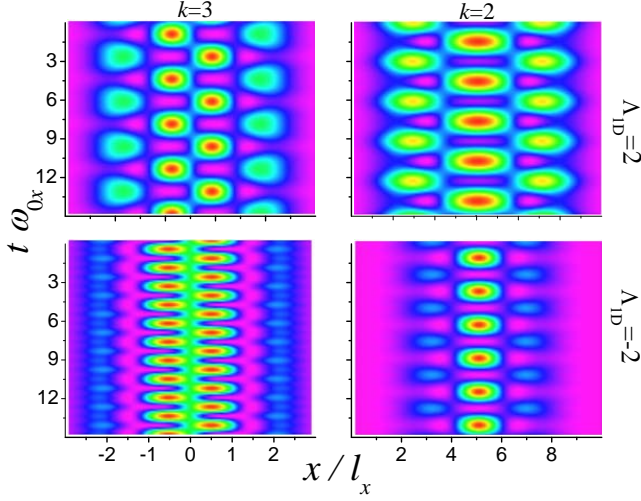


FIG. 5. (Color online): Evolution of the 1D condensate density,  $c_k^{(1D)}(x, t)$ , for the excited state  $\omega_k^{(1D)}$  ( $k = 2$  and  $3$ ) and 1D self-interaction parameter  $\Lambda_{1D} = \pm 2$ .

$x$ -axis quenched according to the exponential behavior  $\exp(-x^2/l_x^2)$ . Moreover, from Fig. 5 it becomes clear that the condensate is stronger localized in space in the case of attractive polariton-polariton interaction (negative sign of  $\Lambda_{1D}$ ).

### B. Normal modes in 1D semi-parabolic potential

Let us now consider a semi-parabolic potential<sup>13,39</sup>

$$V(x) = \begin{cases} 0 & ; \quad x < 0 \\ \frac{1}{2}m\omega_0^2 x^2 & ; \quad 0 < x < \infty \end{cases} . \quad (30)$$

In this case the order parameter must fulfill the boundary conditions  $\psi_0^{(1/2D)}(x=0) = 0$  and  $\psi_0^{(1/2D)} \rightarrow 0$  at  $x \rightarrow \infty$ . The solution of GPE (27) with the semi-parabolic potential (30) yields the following expression for the chemical potential  $\mu_{1/2D}$  obtained up to second order in  $\Lambda_{1D}$  (see Appendix C)

$$\mu_{1/2D} = \omega_{0x} \left( \frac{3}{2} + \frac{3}{2\sqrt{2\pi}} \Lambda_{1D} + C_{1/2} \Lambda_{1D}^2 \right) . \quad (31)$$

The corresponding Bogolyubov's excitation frequencies  $\omega_k^{(1/2D)}$  can be cast as

$$\omega_k^{(1/2D)} = \omega_{0x} \left[ 2k + \frac{\Lambda_{1D}}{\sqrt{2\pi}} \left( -\frac{3}{2} + \frac{4(2k+3/4)(4k)!}{(2k+1)!2^{4k}(2k)!} \right) \Lambda_{1D}^2 \left( \frac{\gamma'_k}{\pi^2} - C_{1/2} \right) \right] ; \quad k = 1, 2, \dots , \quad (32)$$

with  $\gamma'_k$  numeric parameters obtained in Appendix C.

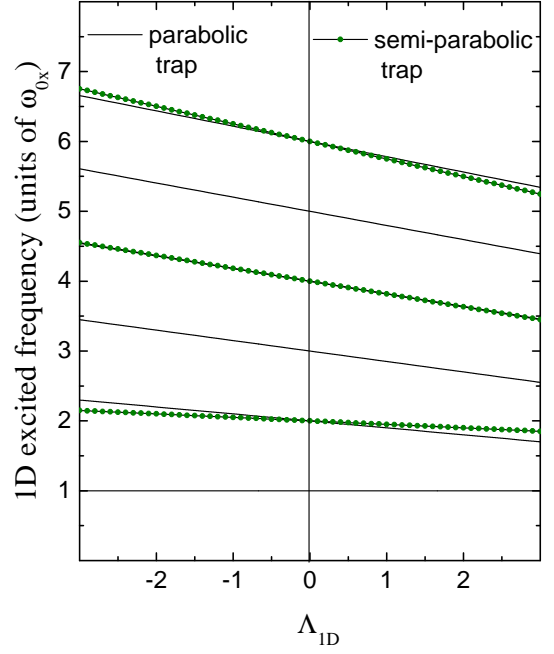


FIG. 6. (Color online): Collective excitation frequencies  $\omega_k^{(1D)}$  (solid lines) and  $\omega_k^{(1/2D)}$  (dot-solid lines) for 1D parabolic and semi-parabolic trap potentials, respectively, as a function of 1D dimensionless parameters  $\Lambda_{1D}$ . Note that  $\omega_1^{(1D)}$  has the frequency value  $\omega_0$  of the harmonic trap (see Ref. 20).

Using the above analytical solutions, the frequencies  $\omega_k^{(1D)}$  and  $\omega_k^{(1/2D)}$  for the first 6 and 3 modes, respectively, *versus* the self-interaction parameter  $\Lambda_{1D}$  (for attractive,  $\Lambda_{1D} < 0$  and repulsive  $\Lambda_{1D} > 0$  polariton-polariton interactions) are represented in Fig. 6. The symmetry of the semi-parabolic trap requires that only odd states exist (see Appendix C). It means that the first excited state corresponds to  $\omega_{k=1}^{(1/2D)}$  and, unlike the case of harmonic potential, its energy depends on  $\Lambda_{1D}$ . This is a consequence of the fact that potential (30) breaks the inversion symmetry and the Kohn's theorem is not valid.

## IV. CONCLUSIONS

In summary, we have studied the two- and one-dimensional Bogolyubov's excitation modes of a Bose-Einstein condensate of exciton-polaritons in 2D in microcavities and microwire-cavities with harmonic traps. In the 2D case we have found eigenenergies and eigenfunctions of the collective modes for two limiting regimes: the weak and strong polariton-polariton interactions. In the weak interaction limit and based on the perturbative method of solution of the non-linear GPE, we derived explicit analytical expressions for the collective excitation frequencies given by Eqs. (12), (29), and (32). In the two-dimensional case, there are two independent subsets

of solutions, with both quantum numbers  $N$  and  $m$  either odd or even, and the corresponding excitation spectrum is ruled by the angular momentum conservation. In all considered cases, the Bogolyubov's frequencies plotted against the self-interaction parameter,  $\lambda$ , show a negative slope. In the case of strong polariton-polariton interaction case, where the Thomas-Fermi approximation is valid, the wave functions and the eigenfrequencies are presented by Eqs. (20) and (21) with the dispersion law  $\lambda$  independent.

We have shown that in 1D traps the polariton-polariton coupling strength is renormalised, and it can be controlled by the confinement potential of the frozen  $y$ -motion (and scales as  $1/L_y$ ), allowing for a modulation of the non-linear cubic term,  $g_1 |\phi_x|^3$ , and, consequently, it affects the spectrum of the excited states. Also, we derived the complete sets of the 2D and 1D excitation modes, which allow for the calculation of a variety of dynamical variables relevant to experiments. In particular, we presented a theory on light scattering by the confined microcavity condensate and calculated, in both considered limits, the spectral dependence of the integrated intensity of a scattered electromagnetic wave. We have calculated the polariton current density associated with the elementary excitations. It is related to the density profile for the excited states (Figs. 2 and 3). We suggest that they are relevant to the experimentally measured real-space spectra distribution for the polariton pendulum (see Figs. 1 and 2 in Refs. 7 and 16) and spatially mapped exciton-polariton condensate wave functions (see Fig. 4 in Ref. 13) are quite well reproduced by the density profiles  $c_k^{(1D)}$  and  $c_k^{(1/2D)}$  ( $k = 1, 2, \dots$ ) given in the Appendices B and C. A good agreement of theory and experiment is found for small values of the  $g_1$  parameter, which corresponds to the experimental setting of Ref. 13.

Finally, we would like to note that, of course, it is an approximation to assume that the polariton condensate is at local equilibrium, i.e. to consider the Gross-Pitaevskii equation in the form (1). However, in the cw non-resonant pumping regime, the actual lifetime of the condensate is significantly increased comparing to the individual polariton lifetime because of the stimulated scattering from an incoherent reservoir. Several experimental works on polariton lasing and BEC indicate that the distribution of exciton polaritons is very close to the equilibrium distribution in these systems. In view of these experimental observations, we believe that the limit of infinitely living condensates is important and experimentally relevant, as it indicates the likely energy spectrum of exciton-polariton condensates in high quality microcavities under non-resonant incoherent cw pumping.

## ACKNOWLEDGMENTS

C.T.-G. and V.L.-R. acknowledge the financial support of Brazilian agencies CNPq and FAPESP. M.V. acknowledges support from the Portuguese Foundation

for Science and Technology through Projects PTDC-FIS-113199-2009 and PEst-C/FIS/UI0607/2013. M.D. is grateful to M. Glazov for valuable discussions and acknowledges the financial support from the Dynasty Foundation, RFBR, and EU projects POLAPHEN and SPANGL4Q. M.D. and A.K. acknowledge Russian Ministry of Education and Science (Contract No. 11.G34.31.0067 with SPbSU).

## Appendix A: 2D eigenmodes

The radial functions for the 2D harmonic oscillator are:  $R_{N,m} = e^{-\frac{\rho^2}{2}} \rho^m L_n^{(m)}(\rho^2) / \sqrt{\mathcal{N}_{N,m}}$ , where  $L_n^{(m)}(z)$  are the Generalized Laguerre polynomials<sup>40</sup>,  $n = (N - m)/2 = 0, 1, \dots$  is the radial number, and  $\mathcal{N}_{N,m} = (\frac{N+m}{2})! / (\frac{N-m}{2})!$  is a normalization constant. Since the perturbation  $\lambda |\psi_0|^2$  in Eq. (3) does not mix states with different angular momenta, the angular dependence of  $|u\rangle$  and  $|v\rangle$  is already known and, in any order of the perturbation theory, the quantum number  $m_z$  is fixed. Moreover, as the radial quantum number is given by  $n = (N - m)/2$ , the solutions can be classified according to parity of the quantum numbers  $N$  and  $m$ , i.e. we have two independent sets of solutions, namely,  $|u_{N,m}^{(I)}\rangle$  and  $|v_{N,m}^{(I)}\rangle$  for  $(N, m)$  even and  $|u_{N,m}^{(II)}\rangle$  and  $|v_{N,m}^{(II)}\rangle$  for  $(N, m)$  odd. After substitution of (11) into (3), the eigenvalue problem is reduced to the system of linear equations:

$$\begin{aligned} & \Lambda \sum_{N_1} \langle R_{N_2,m} | \bar{n}_0 | R_{N_1,m} \rangle (2A_{NN_1} + B_{NN_1}) \\ & = (\varpi_{Nm} - N_2 - 1 + \mu/\omega_0) A_{NN_2}, \end{aligned} \quad (\text{A1})$$

$$\begin{aligned} & -\Lambda \sum_{N_1} \langle R_{N_2,m} | \bar{n}_0 | R_{N_1,m} \rangle (2B_{NN_1} + A_{NN_1}) \\ & = (\varpi_{Nm} + N_2 + 1 - \mu/\omega_0) B_{NN_2}, \end{aligned} \quad (\text{A2})$$

where  $\varpi_{N,m} = \omega_{N,m}/\omega_0$  are the dimensionless Bogolyubov frequencies. The reduced frequencies  $\varpi_{N,m}$ , the coefficients  $A_{NN_1}$  and  $B_{NN_1}$  can be written in a form of Taylor expansions:

$$\begin{aligned} \varpi_{N,m} &= \sum_{i=0}^{\infty} \varpi_{N,m}^{(i)} \Lambda^i, \\ A_{NN_1} [B_{NN_1}] &= \sum_{i=0}^{\infty} A_{NN_1}^{(i)} [B_{NN_1}^{(i)}] \Lambda^i. \end{aligned} \quad (\text{A3})$$

Using the series (A3) and Eqs. (A1) and (A2) at *zeroth order* in  $\Lambda$  we get

$$\varpi_{N,m}^{(0)} = N; B_{NN_2}^{(0)} = 0; A_{NN_2}^{(0)} = \delta_{NN_2}. \quad (\text{A4})$$



Taking the *first order terms* in Eq. (A1) we have

$$2 \langle N_2, m | n^{(0)} | N, m \rangle = \left( \varpi_{N,m}^{(1)} + \frac{1}{2\pi} \right) \delta_{N,N_2} + (N - N_2) A_{NN_2,m}^{(1)}. \quad (\text{A5})$$

Using the condensate distribution density (9) we can write that

$$\langle N_2, m | n^{(0)} | N, m \rangle \equiv C_{N,N_2}^{(0)} = \frac{1}{2\pi \mathcal{N}_{N,m}} \int_0^\infty L_n^{(m)}(t) L_{n_2}^{(m)}(t)^2 \times t^m \exp(-2t) dt.$$

This integral can be calculated in quadrature:<sup>24</sup>

$$C_{N,N_2}^{(0)} = \frac{2^{-n-n_2-m-1} (n+n_2+m)!}{\pi \sqrt{(n+m)! (n_2+m)! n! n_2!}}. \quad (\text{A6})$$

Equation (A5) for  $N_2 = N$  yields:

$$\varpi_{N,m}^{(1)} = \frac{1}{2\pi} \left\{ 2^{-N+1} \left( \binom{N}{(N-m)/2} - 1 \right) \right\}, \quad (\text{A7})$$

and for  $N_2 \neq N$ , it leads to:

$$A_{NN_2,m}^{(1)} = \frac{2}{N - N_2} C_{N,N_2,m}^{(0)}, \quad (\text{A8})$$

while  $A_{NN,m}^{(1)} = 0$  from normalization. In the same way, from (A2), (A4) and (A5), we obtain

$$B_{NN_2,m}^{(1)} = -\frac{1}{N + N_2} C_{N,N_2,m}^{(0)}. \quad (\text{A9})$$

Accordingly, collecting *second order terms* in  $\Lambda$  from (A2) we have,

$$\begin{aligned} & \sum_{N_1} \langle N_2, m | n^{(0)} | N_1, m \rangle \left[ 2A_{NN_1,m}^{(1)} + B_{NN_1,m}^{(1)} \right] \\ & + 2 \langle N_2, m | n^{(1)} | N, m \rangle = (N - N_2) A_{NN_2,m}^{(2)} + \\ & \left( \lambda_{N,m}^{(1)} + E^{(1)} \right) A_{NN_2,m}^{(1)} + \left( \lambda_{N,m}^{(2)} + E^{(2)} \right) \delta_{NN_2}. \end{aligned} \quad (\text{A10})$$

If  $N_2 = N$ , Eq. (A10) reads:

$$\varpi_{N,m}^{(2)} = S_{N,m} + 2C_{N,m}^{(1)} - \frac{1}{2N} \left( C_{N,m}^{(0)} \right)^2 + \frac{3}{8\pi^2} \ln\left(\frac{4}{3}\right), \quad (\text{A11})$$

where

$$S_{N,m} = \sum_{N_1 \neq N} \left[ \left( C_{N,N_1,m}^{(0)} \right)^2 \frac{3N + 5N_1}{(N - N_1)(N + N_1)} \right], \quad (\text{A12})$$

$$C_{N,m}^{(1)} = \frac{1}{2\pi \mathcal{N}_{N,m}} \int_0^\infty \left( L_n^{(m)}(t) \right)^2 t^m F(t) \exp(-2t) dt. \quad (\text{A13})$$

Using the results<sup>24,40</sup>

$$\int_0^\infty t^a \exp(-2t) dt = 2^{-a-1} a!, \quad (\text{A14})$$

$$\int_0^\infty \Gamma(0, t) t^a \exp(-2t) dt = 2^{-a-1} a! B_{2/3}(a+1, 0), \quad (\text{A15})$$

$$\int_0^\infty t^a \ln t \exp(-2t) dt = -2^{-a-1} a! (\gamma - H_a + \ln 2), \quad (\text{A16})$$

with  $H_a$  the  $a$ -th harmonic number, and  $B_x(a, b)$  the Incomplete Beta function, we obtain

$$I_a = \int_0^\infty t^a F \exp(-2t) dt = \frac{a!}{2^{a+2}\pi} \left\{ -\ln 4 + H_a + B_{2/3}(a+1, 0) \right\}.$$

Expanding the Laguerre polynomials as Taylor series<sup>40</sup> follows

$$\left( L_n^{(m)}(t) \right)^2 = \sum_{k,l=0}^n \frac{(-1)^{k+l}}{k!l!} \binom{n+m}{n-k} \binom{n+m}{n-l} t^{k+l}$$

and inserting in Eq. (A13) we have

$$C_{N,m}^{(1)} = \frac{1}{\pi} \frac{n!}{(n+m)!} \sum_{k=0}^n \sum_{l=0}^n \frac{(-1)^{k+l}}{k!l!} \times \binom{n+m}{n-k} \binom{n+m}{n-l} I_{m+k+l}.$$

For the functions  $u_{N,m}$  and  $v_{N,m}$  up to first order in  $\Lambda$  we obtain:

$$u_{N,m} = R_{N,m} + 2\Lambda \sum_{N_2 \neq N} \frac{C_{N,N_2}^{(0)} R_{N_2,m}}{N - N_2}, \quad (\text{A17})$$

$$v_{N,m} = \Lambda \sum_{N_2} \frac{C_{N,N_2}^{(0)} R_{N_2,m}}{N + N_2}. \quad (\text{A18})$$

## Appendix B: 1D eigenmodes for parabolic potential

The concentration  $c_k^{(1D)}$  in the excited state  $k$  is given by

$$c_k^{(1D)} = n_0^{(1D)}(x/l_x) + \delta c_k^{(1D)}(x/l_x, t), \quad (\text{B1})$$

where<sup>37</sup>

$$n_0^{(1D)}(z) = \frac{1}{\sqrt{\pi}} \exp(-z^2) + \Lambda_{1D} \sqrt{\frac{2}{\pi^{3/2}}} \exp(-z^2) \mathcal{F}(z), \quad (\text{B2})$$

$$\mathcal{F}(z) = \int_1^{\sqrt{2}/2} \frac{\exp(-\frac{z^2}{y^2}(1-y^2)) - 1}{1-y^2} dy ,$$

$$\begin{aligned} \delta c_k^{(1D)}(z, t) = & 2 \cos(\omega_k^{(1D)} t) \left( \sqrt{n_0^{(1D)}} \varphi_k(z) \right. \\ & - 2\Lambda_{1D} \varphi_0(z) \left\{ \sum_{m \neq k; m \neq 0} \left[ \frac{1}{m-k} + \frac{1}{2(m+k)} \right] \right. \\ & \left. \left. \times T_{00mk} \varphi_m(z) + \frac{1}{2^2 k} T_{00kk} \varphi_k(z) \right\} \right) , \quad (\text{B3}) \end{aligned}$$

and

$$T_{00mk} = \frac{(-1)^{\frac{k-m}{2}}}{\pi \sqrt{2m!k!}} \Gamma\left(\frac{m+k+1}{2}\right) .$$

Here  $\varphi_k(z)$  is the harmonic oscillator function

$$\varphi_k(z) = \frac{1}{\sqrt{\sqrt{\pi} 2^k k!}} \exp(-\frac{z^2}{2}) H_k(z) , \quad k = 0, 1, 2, \dots \quad (\text{B4})$$

with  $H_l(x)$  denoting the Hermitian polynomial.<sup>40</sup>

### Appendix C: 1D eigenmodes for semi-parabolic potential

Considering the potential (30), the solution of the one-dimensional nonlinear GPE can be sought in terms of the complete set of functions  $\{\varphi_k^{(1/2)}(x/l_x) = \sqrt{2} \varphi_{2k+1}(x/l_x)\}$ . Taking only interaction terms up to second order in  $g_1$ , we obtain for the chemical potential

$$\mu_{1/2D} = \omega_{0x} \left[ \frac{3}{2} + \Lambda_{1/2D} \overline{T_{0000}} - 3\Lambda_{1D}^2 \sum_{p \neq 0} \frac{\overline{T_{000p}^2}}{2p} \right] , \quad (\text{C1})$$

where

$$\overline{T_{mlkp}} = \int_0^\infty \varphi_m^{(1/2)} \varphi_l^{(1/2)} \varphi_k^{(1/2)} \varphi_p^{(1/2)} dx . \quad (\text{C2})$$

From (C2) we have that  $\overline{T_{0000}} = 3/(2\sqrt{2\pi})$  and

$$\overline{T_{000p}} = \sqrt{\frac{2}{\pi}} \frac{(-1)^{p+1}}{2^{2p}} \frac{\sqrt{(2p+1)!}}{p!} \left( \frac{p}{2} - \frac{3}{4} \right) . \quad (\text{C3})$$

Following (C3), the series in Eq. (C1) can be summed up

$$\sum_{p \neq 0} \frac{\overline{T_{000p}^2}}{2p} = \frac{1}{4\pi} \left[ -\frac{3}{2} + \frac{7\sqrt{3}}{9} + 9 \ln \left( 2\sqrt{(2-\sqrt{3})} \right) \right] .$$

For the concentration  $n_0^{(1/2D)}(x/l_x) = \overline{n_0^{(1/2D)}}/l_x$  we have

$$\begin{aligned} \overline{n_0^{(1/2D)}}(z) = & \frac{1}{\sqrt{\pi}} \exp(-z^2) \left[ H_1^2(z) - \Lambda_{1D} \sqrt{\frac{2}{\pi}} \times \right. \\ & \left. H_1(z) \sum_{p \neq 0} \frac{(-1)^{p+1}}{p 2^{3p+1} p!} \left( \frac{p}{2} - \frac{3}{4} \right) H_{2p+1}(z) \right] . \quad (\text{C4}) \end{aligned}$$

Assuming the Bogolyubov's method (2) and employing the expansion  $u_{1/2D}(x)[v_{1/2D}(x)] =$

$$\sum_{k,i=0}^\infty A_k^{(i)(1/2D)} \Lambda_{1/2D}^i \left[ B_k^{(i)(12D)} \Lambda_{1/2D}^i \right] \varphi_k^{(1/2)}(x/l_x)$$

and  $\varpi^{(1/2D)} = \omega_k^{(1/2D)}/\omega_{0x} = \sum_{i=0}^\infty \varpi^{(i)(1/2D)} \Lambda_{1D}^i$ , the collective excitations are described by the linear system equations

$$\begin{aligned} \sum_{i=0}^\infty \Lambda_{1/2D}^i \sum_{k_1} \langle \varphi_k^{(1/2)} | n_0^{(1/2D)} | \varphi_{k_1}^{(1/2)} \rangle \left( 2A_{k_1}^{(i)(1/2D)} + \right. \\ \left. B_{k_1}^{(i)(1/2D)} \right) = \left( \sum_{i=0}^\infty \varpi^{(i)(1/2D)} \Lambda_{1D}^i - 2k \right. \\ \left. - \frac{3}{2} + \frac{\mu_{1/2D}}{\omega_{0x}} \right) \Lambda_{1D}^k A_k^{(i)(1/2D)} , \quad (\text{C5}) \end{aligned}$$

and similar equations but changing  $A_{k_1}^{(i)(1/2D)} \Leftrightarrow B_{k_1}^{(i)(1/2D)}$ . From these system equations we get at *zeroth order* in  $\Lambda_{1D}$  the  $\varpi_k^{(0)(1/2D)} = 2k$  and at *first order*,

$$\varpi_k^{(1)(1/2D)} = \Lambda_{1D} \left[ -\frac{3}{2\sqrt{2\pi}} + 2\overline{T_{00kk}} \right] ,$$

where

$$\overline{T_{00kk}} = \frac{2(2k+3/4)}{\sqrt{2\pi}(2k+1)!} \frac{(4k)!}{2^{4k}(2k)!} .$$

For the second order immediately follows

$$\begin{aligned} \omega_k^{(2)(1/2D)} = & -\mu_{1/2D}^{(2)} + 4\Lambda_{1D}^2 \left[ -\sqrt{\frac{2}{\pi}} \times \right. \\ & \sum_{p \neq 0} \frac{(-1)^{p+1} \sqrt{(2p+1)!}}{2^{2p} 2pp!} \left( \frac{p}{2} - \frac{3}{4} \right) \overline{T_{0pkk}} \\ & - \frac{1}{2} \sum_{p \neq 0; p \neq k} \left( \frac{1}{p-k} + \frac{1}{4(p+k)} \right) \overline{T_{00pk}^2} \\ & \left. - \frac{1}{16k} \overline{T_{00kk}^2} \right] ; \quad k = 1, 2, \dots , \quad (\text{C6}) \end{aligned}$$

with

$$\overline{T_{00kp}} = \frac{(-1)^{k-p}}{\pi} \frac{\sqrt{2}\Gamma(k+p+1/2)}{\sqrt{(2k+1)!(2p+1)!}} \times \left[ \frac{1}{4} - (k-p)^2 + k + p + \frac{1}{2} \right] \quad (C7)$$

and

$$\overline{T_{0kkp}} = \frac{1}{\pi^2\sqrt{2}} \frac{\Gamma^2(p+1/2)\Gamma(2k-p+1/2)}{(2k+1)!\sqrt{(2p+1)!}} \times (2p+1)[2+4k-2p] \quad (C8)$$

According to Eqs. (C6)-(C8) we finally obtain

$$\omega_k^{(2)(1/2D)} = \Lambda_{1D}^2 \left( \frac{\gamma'_k}{\pi^2} - C_{1/2} \right), \quad (C9)$$

$$\text{with } C_{1/2} = -\frac{3}{4\pi} \left[ -\frac{3}{2} + \frac{7\sqrt{3}}{9} + 9 \ln 2 \sqrt{(2-\sqrt{3})} \right]$$

$$\gamma'_k = \frac{4}{\sqrt{\pi}} \sum_{p \neq 0} \left[ \frac{(-1)^{p+1} \left(\frac{3}{2} - p\right) \Gamma^2(p+1/2)}{2^{2p+1} (2k+1)!} \times \frac{\Gamma(2k-p+1/2)(2p+1)(1+2k-p)}{pp!} \right] - \sum_{p \neq 0; m \neq k} \left[ \left( \frac{1}{m+k} + \frac{4}{m-k} \right) \times \frac{\Gamma^2(p+\frac{1}{2}+k)}{(2k+1)!} - \frac{1}{(2p+1)!} \left[ \frac{3}{4} - (k-p)^2 + k + p \right]^2 \right] - \frac{1}{4} \frac{\Gamma^2(2k+\frac{1}{2}) \left(\frac{3}{4} + 2k\right)^2}{2k[(2k+1)!]^2}. \quad (C10)$$

For an evaluation of the concentration  $c_k^{(1/2D)}$  we just need to substitute in Eqs. (B1) and (B3)  $n_0^{(1D)}(z) \rightarrow n_0^{(1/2D)}(z)$ ,  $\omega_k^{(1D)} \rightarrow \omega_k^{(1/2D)}$ ,  $\varphi_k \rightarrow \varphi_k^{(1/2)}$  and  $T_{00kp} \rightarrow \overline{T_{00kp}}$ .

- 
- <sup>1</sup> A. Amo, D. Sanvitto, F. P. Laussy, D. Ballarini, E. del Valle, M. D. Martin, A. Lemaître, J. Bloch, D. N. Krizhanovskii, M. S. Skolnick, C. Tejedor, and L. Viña, *Nature* **457**, 291 (2009).
- <sup>2</sup> J. Keeling and N. G. Berloff, *Nature* **457**, 273(2009).
- <sup>3</sup> D. Sarchi and V. Savona, *Phys. Rev. B* **77**, 045304 (2008).
- <sup>4</sup> D. Sanvitto, F. M. Marchetti, M. H. Szymańska, G. Tosi, M. Baudisch, F. P. Laussy, D. N. Krizhanovskii, M. S. Skolnick, L. Marrucci, A. Lemaître, J. Bloch, C. Tejedor and L. Viña, *Nature Phys.* **6**, 527 (2010).
- <sup>5</sup> K. G. Lagoudakis, T. Ostatnický, A. V. Kavokin, Y. G. Rubo, R. André, and B. Deveaud-Plédran, *Science* **326**, 974 (2009).
- <sup>6</sup> T. C. H. Liew, M. M. Glazov, K.V. Kavokin, I. A. Shelykh, M. A. Kaliteevski, and A.V. Kavokin, *Phys. Rev. Lett.* **110**, 047402 (2013).
- <sup>7</sup> G. Tosi, G. Christmann, N. G. Berloff, P. Tsotsis, T. Gao, Z. Hatzopoulos, P. G. Savvidis, and J. J. Baumberg, *Nature Physics* **8**, 190 (2012).
- <sup>8</sup> N. N. Bogolyubov, *J. Phys. USSR* **11**, 23(1947).
- <sup>9</sup> M. H. Anderson, et al., *Science* **269**, 198 (1995).
- <sup>10</sup> S. Utsunomiya, L. Tian, G. Roumpos, C. W. Lai, N. Kumada, T. Fujisawa, M. Kuwata-Gonokami, A. Löffler, S. Höfling, A. Forchel, and Y. Yamamoto, *Nature Physics*, **4**, 702 (2008).
- <sup>11</sup> M. Assmann, J.-S. Tempel, F. veit, M. Bayer, A. Rahimi-Iman, A. Löffler, S. Hörling, S. Reitzenstein, L. Worschech, and A. Forchel, *PNAS* **108**, 1804 (2011).
- <sup>12</sup> D. Bajoni, E. Peter, P. Senellart, J. L. Smirri, I. Sagnes, A. Lemaître, and J. Bloch, *Appl. Phys. Lett.* **90**, 051107 (2007).
- <sup>13</sup> E. Wertz, L. Ferrier, D. D. Solnyshkov, R. Johne, D. Sanvitto, A. Lemaître, I. Sagnes, R. Grousson, A. V. Kavokin, P. Senellart, G. Malpuech and J. Bloch, *Nature Physics* **6**, 860 (2010).
- <sup>14</sup> A. Amo, S. Pigeon, C. Adrados, R. Houdré, E. Giacobino, C. Ciuti, and A. Bramati, *Phys. Rev. B* **82**, 081301(R) (2010).
- <sup>15</sup> M. Wouters, T. C. H. Liew, and V. Savona, *Phys. Rev. B* **82**, 245315 (2010).
- <sup>16</sup> A. Kavokin, *Nature Physics* **8**, 183 (2012).
- <sup>17</sup> Ting-Wei Chen, Szu-Cheng Cheng and Wen-Feng Hsieh, *Phys. Rev. B* **88**, 184502 (2013).
- <sup>18</sup> C. Trallero-Giner, T. C. H. Liew, and A. V. Kavokin, *Phys. Rev. B* **82**, 165421 (2010).
- <sup>19</sup> C. Ciuti, V. Savona, C. Piermarocchi, A. Quattropani, and P. Schwendimann, *Phys. Rev. B* **58**, 7926 (1998).
- <sup>20</sup> L. Pitaevskii and S. Stringari, *Bose-Einstein Condensation* (Clarendon Press, Oxford, 2003).
- <sup>21</sup> L. You, W. Hoston, and M. Lewenstein, *Phys. Rev. A* **55**, R1581 (1997).
- <sup>22</sup> S. Stringari, *Phys. Rev. Lett.* **77**, 2360 (1996).
- <sup>23</sup> Y. N. Fernández, M. I. Vasilevskiy, C. Trallero-Giner, and A. Kavokin, *Phys. Rev. B* **87**, 195441 (2013).
- <sup>24</sup> I. S. Gradshteyn and I. M. Ryzhik, *Tables of Integrals, Series and Products* (Academic, New York, 1980).
- <sup>25</sup> G. W. Gibbons and C. N. Pope, *Ann. Phys.* **326**, 1760 (2011).
- <sup>26</sup> M. Edwards, P. A. Ruprecht, K. Burnett, R. J. Dodd, and C. W. Clark, *Phys. Rev. Lett.* **77** 1671 (1996).
- <sup>27</sup> H. Mathieu, P. Lefebvre, J. Allegre, B. Gil, and A. Regreny, *Phys. Rev. B* **36**, 6581 (1987).
- <sup>28</sup> J. R. Abo-Shaer, C. Raman, J. M. Vogels, and W. Ketterle, *Science* **292**, 476 (2001).
- <sup>29</sup> Tomas-Fermi limit becomes good approach for the GPE if the dimensionless parameter  $\Lambda \geq 25$  (see Refs. 18 and 23). For the GaAs/AlAs microcavities this value can be achieved if the exciton-photon detuning parameter  $\delta \approx 0$

meV and  $\mathcal{N}$  larger than  $2.5 \times 10^5$ .

- <sup>30</sup> T. P. Pearsall, Appl. Phys. Lett. **60**, 1712 (1992).
- <sup>31</sup> E. D. Kim, A. Majumdar, H. Kim, P. Petroff, and J. Vuckovic, Appl. Phys. Lett. **97**, 053111 (2010).
- <sup>32</sup> M. J. Collett and C. W. Gardiner, Phys. Rev. A **30**, 1386 (1984).
- <sup>33</sup> D. F. Walls and G. J. Milburn, *Quantum Optics* (Springer-Verlag, Berlin 1995)
- <sup>34</sup> See Refs. 35 for general discussion.
- <sup>35</sup> A. E. Muryshv, G. V. Shlyapnikov, W. Ertmer, K. Sengstock, and M. Lewenstein, Phys. Rev. Lett. **89**, 110401 (2002); L. Khaykovich and B. A. Malomed, Phys. Rev. A **74**, 023607 (2006); C. Trallero-Giner, R. Cipelatti, and T. C. H. Liew, Eur. Phys. J. D **67**, 143 (2013).
- <sup>36</sup> Notice that in Refs. 13 and 15 for the solution of 1D equations the authors employed a 2D value for polariton-polariton interaction constant  $\lambda$ . This is equivalent to normalized the 1D wave function to width of the wire,  $L_y$ , which leads to inaccurate value of the 1D polariton-polariton interaction constant  $g_1 = \mathcal{N}\lambda/L_y$ .
- <sup>37</sup> C. Trallero-Giner, Victor Lopez-Richard, Ming-Chiang Chung, and Andreas Buchleitner, Phys. Rev. A **79**, 195441 (2009).
- <sup>38</sup> C. Trallero-Giner, V. López-Richard, Y. Núñez-Fernández, M. Oliva, G.E. Marques, and M.C. Chung, Eur. Phys. J. D **66**, 177 (2012).
- <sup>39</sup> L. Ferrier, E. Wertz, R. Johne, D. D. Solnyshkov, P. Senellart, I. Sagnes, A. Lemaître, G. Malpuech, and J. Bloch, Phys. Rev. Lett. **106**, 126401 (2011).
- <sup>40</sup> M. Abramowitz and I. Stegun, eds., *Handbook of Mathematical Functions* (Dover, New York, 1972).